Quantum information and quantum contextuality in Grothendieck's coset space

Michel Planat

Institut FEMTO-ST, CNRS, 15 B Avenue des Montboucons, F-25044 Besançon
(michel.planat@femto-st.fr)

SEAMS School, Kuala Lampur: 5 November 2015

Abstract[1,2,3]

- In quantum mechanics, **Bell's theorem** forbids local hidden variable theories (that were hoped by A. Einstein) while **Kochen-Specker theorem** also forbids non-contextual theories.

  Mermin's square and pentagram (from two- and three-qubit Pauli groups) provide a finite geometrical interpretation of these theorems.
- I show how these (and higher order) geometries and **the related contextuality** arise from Grothendieck's dessins d'enfants and the structure of the corresponding cosets. I introduce a measure of geometrical contextuality.

---

[1] M. Planat, On small proofs of the Bell-Kochen-Specker theorem for two, three and four qubits, *EPJ Plus* **127**, 86 (2012).

[2] M. Planat, A. Giorgetti, F. Holweck and M. Saniga, Quantum contextual finite geometries from dessins d'enfants, *Int. J. Geom. Meth. in Mod. Phys.* **12** 1550067 (2015).

[3] M. Planat, Geometry of contextuality from Grothendieck's coset space, *Quant. Inf. Proc.* **14**, 2563-2575 (2015).

The square geometry of Bell's theorem

In a theory in which parameters are added to quantum mechanics to determine the results of individual measurements, without changing the statistical predictions, there must be a mechanism whereby the setting of one measuring device can influence the reading of another instrument, however remote (Bell 1964).

- Suppose we have four observables σ_i, $i = 1, 2, 3, 4$, taking values in $\{-1, 1\}$, of which Bob can measure (σ_1, σ_3) and Alice (σ_2, σ_4). The **Bell-CHSH approach to quantum contextuality/non-locality** consists of defining the number

$$C = \sigma_2(\sigma_1 + \sigma_3) + \sigma_4(\sigma_3 - \sigma_1) = \pm 2$$

and observing the (so-called Bell-CHSH) inequality [4]

$$|\langle\sigma_1\sigma_2\rangle + \langle\sigma_2\sigma_3\rangle + \langle\sigma_3\sigma_4\rangle - \langle\sigma_4\sigma_1\rangle| \leq 2,$$

where $\langle\rangle$ here means that we are taking averages over many experiments.

[4] A. Peres, Quantum theory: concepts and methods (Kluwer, 1995).

The square geometry of Bell's theorem: 2

- This inequality holds for any dichotomic random variables σ_i. **Bell's theorem** states that the inequality is violated if one considers **quantum observables with dichotomic eigenvalues**. An example is

$$\sigma_1 = I \otimes X,\ \sigma_2 = X \otimes I,\ \sigma_3 = I \otimes Z,\ \sigma_4 = Z \otimes I$$

$$C^2 = 4 * I + [\sigma_1, \sigma_3][\sigma_2, \sigma_4] = 4 \begin{pmatrix} 1 & . & . & 1 \\ . & 1 & \bar{1} & . \\ . & \bar{1} & 1 & . \\ 1 & . & . & 1 \end{pmatrix}$$

has eigenvalues 0 and 8, both with multiplicity 2 ($\bar{1} \equiv -1$). Using the norm $||A|| = sup(||A\psi||/||\psi||)$,$\psi \in \mathcal{H}$, one arrives at the **maximal violation of the Bell-CHSH inequality** $||C|| = 2\sqrt{2}$.

The point-line incidence geometry associated with our four observables is one of the simplest, that of a **square**. There are 90 distinct squares among two-qubit observables and 30240 when three-qubit labeling is employed, each yielding a maximal violation of the Bell-CHSH inequality.

Peres, 1995: *There is no escape from nonlocality. The experimental violation of Bell's inequality leaves only two possibilities:* **either** *some simple physical observers (such as correlated photon pairs) are essentially nonlocal,* **or** *it is forbidden to consider simultaneously the possible outcomes of mutually exclusive experiments, even though any one of these experiments is actually realizable. The second alternative effectively rules out the introduction of exophysical automatons with a random behavior-let alone observers endowed with free will. If you are willing to accept that option,* **then it is the entire universe which is an indivisible, nonlocal entity.**

The Bell-Kochen-Specker theorem: 1

- The **Bell-Kochen-Specker proof** demonstrates the impossibility of Einstein's assumption, made in the famous Einstein-Podolsky-Rosen paper [5], that quantum mechanical observables represent 'elements of physical reality'. More specifically, the theorem **excludes hidden variable theories** that require elements of physical reality to be **non-contextual** (i.e. independent of the measurement arrangement) [6]
- **Essence of the BKS proof**: even for compatible observables A and B with values $v(A)$ and $v(B)$, the equations $v(aA + bB) = av(A) + bv(B)$ $(a, b \in \mathbb{R})$ or $v(AB) = v(A)v(B)$ may be violated.

[5] A. Einstein, B. Podolsky and N. Rosen, "Can quantum-mechanical description of physical reality be considered complete?" Phys. Rev. 47, 77780 (1935).

[6] Kochen S. and Specker E. P. 1967 The problem of hidden variables in quantum mechanics *J. Math. Mech.* **17** 59–87.

The Bell-Kochen-Specker theorem: 2

- A **non-coloring BKS proof** consists of a finite set of rays/vectors that cannot be assigned truth values (1 for true, 0 for false) in such a way that (i) one ray in each complete orthonormal basis is true and (ii) no two orthogonal (that is, mutually compatible) projectors are both true.

  The smallest state-independent proofs in three dimensions are of the $31 - 17$ type (31 rays located on 17 orthogonal triads)[7].

- A **parity proof of BKS theorem** is a set of v rays that form l bases (l odd) such that each ray occurs an even number of times over these bases.

  The **smallest BKS proof** in dimension 4 (resp. 8) is a parity proof and corresponds to arrangements of real states arising from the two-qubit (resp. three-qubit) **Pauli group**, more specifically as eigenstates of operators forming Mermin's square (resp. Mermin's pentagram) [8].

[7] Peres A. 1993 *Quantum theory: concepts and methods* (Kluwer.

[8] Cabello A., Estebaranz J. M. and García-Alcaine G. 1996 Bell-Kochen-Specker theorem: A proof with 18 vectors *Phys. Lett. A* **212** 183–187.

The distance between the maximal orthonormal bases

Apart from the use of standard graph theoretical tools for characterizing the ray/base symmetries, we shall employ a useful signature of the proofs in terms of **Bengtsson's distance** D_{ab} between two orthonormal bases a and b defined as [9]

$$D_{ab}^2 = 1 - \frac{1}{d-1} \sum_{i,j}^{d} \left(|\langle a_i | b_j \rangle|^2 - \frac{1}{d} \right)^2 .$$

The distance (1) vanishes when the bases are the same and is maximal (equal to unity) when the two bases a and b are mutually unbiased, $|\langle a_i | b_j \rangle|^2 = 1/d$, and only then. We shall see that the bases of a BKS proof employ a selected set of distances which seems to be a universal feature of the proof.

[9] Raynal P., Lü X. and Englert B.-G. 2011 Mutually unbiased bases in six dimensions: the four most distant bases *Phys. Rev. A* **83** 062303.

The Peres-Mermin square: an operator parity proof of 2QB BKS theorem [10]

We denote by X, Z and Y the **Pauli spin matrices** in x, y and z directions, and the tensor product is not explicit, i. e. for two qubits one denotes $Z_1 = Z \otimes I$, $Z_2 = I \otimes Z$ and $ZZ = Z \otimes Z$, for three qubits one denotes $Z_1 = Z \otimes I \otimes I$ and so on.

$$\begin{array}{ccc}
| & | & || \\
-Z_1- & Z_2- & ZZ-_{I} \\
| & | & || \\
-X_2- & X_1- & XX-_{I} \\
| & | & || \\
-ZX- & XZ- & YY-_{I} \\
|_{I} & |_{I} & ||_{-I}
\end{array}$$

There is **no way** of assigning multiplicative properties to the eigenvalues ± 1 of the nine operators while still keeping the same multiplicative properties for the operators.

[10] Mermin N. D. 1993 Hidden variables and the two theorems of John Bell *Rev. Mod. Phys.* **65** 803-815.

2QB real eigenvectors and their maximal orthonormal bases

- 6 (operator) bases $\times 4$ (eigenstates) $=$ 24 real eigenstates/rays

$$\begin{gathered}1:[1000],\quad 2:[0100],\quad 3:[0010],\quad 4:[0001],\quad 5:[1111],\quad 6:[11\bar{1}\bar{1}]\\ 7:[1\bar{1}1\bar{1}],\quad 8:[1\bar{1}\bar{1}1],\quad 9:[1\bar{1}\bar{1}\bar{1}],\quad 10:[1\bar{1}11],\quad 11:[11\bar{1}1],\quad 12:[111\bar{1}]\\ 13:[1100],\quad 14:[1\bar{1}00],\quad 15:[0011],\quad 16:[001\bar{1}],\quad 17:[0101],\quad 18:[010\bar{1}]\\ 19;[1010],\quad 20:[10\bar{1}0],\quad 21:[100\bar{1}],\quad 22:[1001],\quad 23:[01\bar{1}0],\quad 24:[0110]\end{gathered} \tag{1}$$

- 24 complete orthogonal bases (numbered in blue)

$$\begin{gathered}1\colon\{1,2,3,4\},2\colon\{5,6,7,8\},3\colon\{9,10,11,12\},4\colon\{13,14,15,16\},\\ 5\colon\{17,18,19,20\},6\colon\{21,22,23,24\},7\colon\{1,2,15,16\},8\colon\{1,3,17,18\},\\ 9\colon\{1,4,23,24\},10\colon\{2,3,21,22\},11\colon\{2,4,19,20\},12\colon\{3,4,13,14\},\\ 13\colon\{5,6,14,16\},14\colon\{5,7,18,20\},15\colon\{5,8,21,23\},16\colon\{6,7,22,24\},\\ 17\colon\{6,8,17,19\},18\colon\{7,8,13,15\},19\colon\{9,10,13,16\},20\colon\{9,11,18,19\},\\ 21\colon\{9,12,22,23\},22\colon\{10,11,21,24\},23\colon\{10,12,17,20\},24\colon\{11,12,14,15\}\end{gathered} \tag{2}$$

The diagram for a $18-9$ proof

The diagram for the $18-9$ proof is simply a 3×3 square. **There are** 18 **(distinct) edges that encode the** 18 **rays**, a selected vertex/base of the graph is encoded by the union of the four edges/rays that are adjacent to it.

$$\begin{array}{ccc}
\begin{pmatrix} 1 & 2 \\ 15 & 16 \end{pmatrix} -1- & \begin{pmatrix} 1 & 3 \\ 17 & 18 \end{pmatrix} -3- & \begin{pmatrix} 2 & 3 \\ 21 & 22 \end{pmatrix} -2 \\
|_{16} & |_{18} & |_{22} \\
\begin{pmatrix} 5 & 6 \\ 14 & 16 \end{pmatrix} -5- & \begin{pmatrix} 5 & 7 \\ 18 & 20 \end{pmatrix} -7- & \begin{pmatrix} 6 & 7 \\ 22 & 24 \end{pmatrix} -6 \\
|_{14} & |_{20} & |_{24} \\
\begin{pmatrix} 11 & 12 \\ 14 & 15 \end{pmatrix} -12- & \begin{pmatrix} 10 & 12 \\ 17 & 20 \end{pmatrix} -10- & \begin{pmatrix} 10 & 11 \\ 21 & 24 \end{pmatrix} -11 \\
|_{15} & |_{17} & |_{21}
\end{array}$$

As for the **distances** between the bases, two bases located in the same row (or the same column) have distance $a_2 = \sqrt{7/12}$, while two bases not in the same row (or column) have distance $a_4 = \sqrt{5/6} > a_2$.

Distance signature of the 2QB proofs

the **five distances** involved

$$D = \{a_1, a_2, a_3, a_4, a_5\} = \{\frac{1}{\sqrt{3}}, \frac{\sqrt{7}}{\sqrt{12}}, \frac{\sqrt{2}}{\sqrt{3}}, \frac{\sqrt{5}}{\sqrt{6}}, 1\}.$$

proof $v-l$	# proofs	a_1	a_2	a_3	a_4	a_5
$24-15$	16	18	18	9	54	6
$22-13A$	96	12	18	3	42	3
$22-13B$	144	12	18	4	42	2
$20-11A$	96	6	18	0	30	1
$20-11B$	144	6	18	1	30	0
$18-9$	16	0	18	0	18	0

- The histogram of distances. The symmetry group of Mermin's graph is $G_{72} = \mathbb{Z}_3^2 \rtimes D_4$. It governs most of the above 2^9 proofs although there also exist some extra abelian symmetries. Another nice geometrical display of the proofs is in *Waegell M. and Aravind P. K. 2011 Parity proofs of the Kochen-Specker theorem based on the* 24 *rays of Peres Found. Phys.* **41** *1786-1799.*).

The Mermin'spentagram: an operator parity proof of 3QB BKS theorem [11]

As for the 2QB MS, **no way** of assigning multiplicative properties to the eigenvalues ± 1 while keeping the same multiplicative properties for the 10 operators. (Also *Saniga M. and Lévay P. 2012 Mermin's pentagram as an ovoid of* $PG(3,2)$ *EPL* **97** *50006).*

$$
\begin{array}{cccc}
| & | & | & | \\
Z_1 & Z_1 & X_1 & X_1 \\
| & | & | & | \\
Z_2 & X_2 & Z_2 & X_2 \\
| & | & | & | \\
Z_3 & X_3 & X_3 & Z_3 \\
| & | & | & | \\
= ZZZ = & ZXX = & XZX = & XXZ = -_I \\
|_I & |_I & |_I & |_I
\end{array}
$$

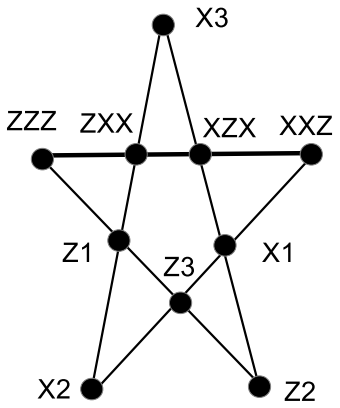

3QB real eigenvectors and their maximal orthonormal bases

$$1 : [10000000], 2 : [01000000], 3 : [00100000], 4 : [00010000], 5 : [00001000],$$
$$6 : [00000100], 7 : [00000010], 8 : [00000001], 9 : [11110000], 10 : [11\bar{1}\bar{1}0000],$$
$$11 : [1\bar{1}1\bar{1}0000], 12 : [1\bar{1}\bar{1}10000], 13 : [00001111], 14 : [00001\bar{1}\bar{1}\bar{1}], 15 : [0000\bar{1}1\bar{1}\bar{1}],$$
$$16 : [0000\bar{1}\bar{1}\bar{1}1], 17 : [11001100], 18 : [1100\bar{1}\bar{1}00], 19 : [1\bar{1}001\bar{1}00], 20 : [1\bar{1}00\bar{1}100],$$
$$21 : [00110011], 22 : [00110\bar{1}\bar{1}], 23 : [001\bar{1}001\bar{1}], 24 : [001\bar{1}00\bar{1}1], 25 : [10101010],$$
$$26 : [1010\bar{1}0\bar{1}0], 27 : [10\bar{1}010\bar{1}0], 28 : [10\bar{1}0\bar{1}010], 29 : [01010101], 30 : [0101\bar{0}\bar{1}0\bar{1}],$$
$$31 : [010\bar{1}010\bar{1}], 32 : [010\bar{1}0\bar{1}01], 33 : [10010\bar{1}\bar{1}0], 34 : [100\bar{1}0110], 35 : [1001\bar{0}\bar{1}10],$$
$$36 : [100\bar{1}0\bar{1}\bar{1}0], 37 : [0110\bar{1}001], 38 : [01\bar{1}01001], 39 : [01\bar{1}0\bar{1}00\bar{1}], 40 : [0110100\bar{1}].$$

The $5 \times 8 = 40$ real rays form 25 maximal orthogonal bases.

Distance signature of the 3QB proofs

$$D = \{a_1, a_2, a_3\} = \{\frac{\sqrt{3}}{\sqrt{7}}, \frac{\sqrt{9}}{\sqrt{14}}, \frac{\sqrt{6}}{\sqrt{7}}\}$$

proof $v - l$	# proofs	a_1	a_2	a_3
$40 - 15$	64	20	30	55
$38 - 13$	640	12	30	26
$36 - 11$	320	4	30	21

- The histogram of distances for the 2^{10} 3QB BKS proofs.

A schematic diagram for a $36-11$ proof

- Let us look at a $36-11$ parity proof. The 11 bases are displayed as a **pentagram** plus the isolated base 1.

$$
\begin{array}{ccccccccccc}
 & & & & 2 & & & & & & \\
6 & - & & 7 & - & 8 & & - & 9 & == & 1 \\
 & & 10 & & & & 11 & & & & \\
 & & & & 3 & & & & & & \\
 & 4 & & & & & & 5 & & &
\end{array}
$$

- Two adjacent bases of the pentagram have **two rays** in common. The reference base has with each of the bases on the horizontal line of the pentagram **four rays** in common and is disjoint from any other base. Each line of the pentagram shares a set of four rays that is **disjoint** from the set of four rays shared by another line. The automorphism group of this configuration is isomorphic to S_5.
- The maximal distance, a_3, is that between two disjoint bases, and amounts to $\sqrt{6/7}$. The intermediate distance, $a_2 = \sqrt{9/14}$, occurs between two bases located in any line of the pentagram. Finally, the shortest distance, $a_1 = \sqrt{3/7}$, is that between the reference base and each of the four bases on the horizontal line of the pentagram. Similar diagrams can be produced for any proof.

Grothendieck famous sentence[12]

Whereas in my research before 1970, *my attention was systematically directed towards objects of maximal generality, in order to uncover a general language adequate for the world of algebraic geometry, and I never restricted myself to algebraic curves except when strictly necessary (notably in etale cohomology), preferring to develop pass-key techniques and statements valid in all dimensions and in every place (I mean, over all base schemes, or even base ringed topoi...), here I was brought back,* **via objects so simple that a child learns them while playing, to the beginnings and origins of algebraic geometry**, *familiar to Riemann and his followers!*

[12] A. Grothendieck, Sketch of a programme, written in 1984 and reprinted with translation in L. Schneps and P. Lochak (eds.), Geometric Galois Actions: 1. Around Grothendieck's Esquisse d'un Programme, and 2. The inverse Galois problem, Moduli Spaces and Mapping Class Groups (Cambridge Press, 1997).

The two-generator free group, its subgroups and the cosets

- Let $F = \langle a, b \rangle$ be the free group on two generators. Elements in the group are **words** u, and $uu^{-1} = e$. We restrict to the free group $G = \langle a, b \mid b^2 = 1 \rangle$. The **index** $n := |G : H|$ of a subgroup H in G counts the number of cosets/copies of H that fill up G. A right coset with respect to an element $g \in G$ is defined as $Hg = \{hg : h \in H\}$. The set of right cosets **partitions** G.
- A transversal is an indexed set of (right) coset representatives for H in G, and the **coset table** expresses the action of a, b on them. (Coxeter-Todd algorithm). Under a and b, the indexed coset representatives are mapped to a two-generator permutation group $P = \langle g_0, g_1 \rangle$.
- The latter is a **map** on a **compact orientable surface** that is, a triple (g_0, g_1, g_∞) with $g_0 g_1 g_\infty = 1$, from which V vertices, E edges and F faces are defined by the cycles of g_0, g_1 and g_∞. The map may be seen as a bicolored **(hyper)map** $\mathcal{D}$ with B black and W white vertices, adjacent vertices always have opposite color and the segments are the n edges. The dessin $\mathcal{D}$ is endowed a natural topological structure with **Euler characteristic** $2 - 2g = B + W + F - n$.

Belyi's theorem

- Belyi's theorem: a dessin may also been seen as a compact Riemann surface $\mathcal{S}$ defined over the field $\bar{\mathbb{Q}}$ of algebraic numbers. The Belyi function is $f : \mathcal{S} \to \mathbb{P}^1$, where $\mathbb{P}^1$ is the Riemann sphere with at most three branching values.

  Technically, given $f(x)$, a rational function of the complex variable x, a **critical point** of f is a root of its derivative and a **critical value** of f is the value of f at the critical point.

- The Belyi function $f(x)$ corresponding to a dessin is of degree n if $\mathcal{D}$ may be embedded into the Riemann sphere $\hat{\mathbb{C}}$ and (i) the **black** vertices are the roots of $f(x) = 0$ with multiplicity equal to the degree of the corresponding (black) vertex, (ii) the **white** vertices are the roots of $f(x) = 1$ with multiplicity equal to the degree of the corresponding (white) vertex, (iii) the bicolored graph is the **preimage** of the segment $[0, 1]$, that is $\mathcal{D} = f^{-1}([0, 1])$, (iv) there exists **a single pole** of $f(x)$, i. e. a root of $f(x) = \infty$ **at each face**, the multiplicity of the pole equal to the degree of the face, and, finally, (v) besides 0, 1 and ∞, there are **no other critical values** of f.

A stabilized point/line geometry

- Coset graphs and the related dessins provide a coordinatization to many point-line geometries occuring in the investigation of commutation of quantum observables.

  Taking the **permutation group** P (thus a dessin $\mathcal{D}$) corresponding to a subgroup H of G, one proceeds by first listing the m non-isomorphic subgroups S_m **stabilizing a pair of elements/cosets**.

  Then, given a S_m, all points on a line of the putative geometry $\mathcal{G}_m$ should share the **same** two-point stabilizer subgroup of P. The lines of a $\mathcal{G}_m$ are thus distinguished by their (isomorphic) stabilizers acting on different G-sets. Doing this, the **cosets happen to coordinatize** the edges of the $\mathcal{D}$ and, at the same time, the vertices of the resulting geometries $\mathcal{G}_m$.

Bell's theorem from the square geometry: 1

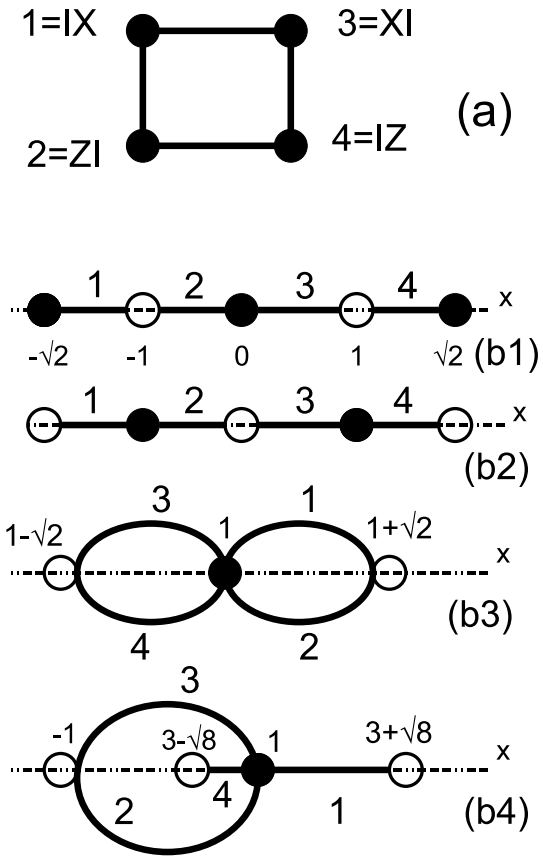

- A simple observable proof of Bell's theorem embodied in the geometry of a square (a) and four associated *dessins d'enfants*, (b_1) to (b_4).

Bell's theorem from the square geometry: 2

- **Dessin (b1)**: signature $s = (B, W, F, g) = (3, 2, 1, 0)$, group $P = \langle (2,3), (1,2)(3,4) \rangle$, cycle structure $[2^1 1^2, 2^2, 4^1]$ and Belyi function $f(x) = x^2(2 - x^2)$. The critical points are $x \in \{-1, 1, 0\}$ and the critical values are $\{1, 1, 0\}$. Preimage of the value 0 (solutions of $f(x) = 0$) corresponds to black vertices at $x \in \{-\sqrt{2}, \sqrt{2}, 0\}$. Preimage of the value 1 (solutions of $f(x) = 1$) corresponds to the white vertices at $x = \pm 1$.
- **Dessin (b2)**: $s = (2, 3, 1, 0)$, $P = \langle (1,2)(3,4), (2,3) \rangle$, cycles $[2^2, 2^1 1^2, 4^1]$ and Belyi function $f(x) = (x^2 - 1)^2$.
- **Dessin (b3)**: Belyi function $f(x) = \frac{(x-1)^4}{4x(x-2)}$. As $f'(x) = \frac{(x-1)^3(x^2-2x-1)}{2(x-2)^2x^2}$, its critical points lie at $x = 1$ (where $f(1) = 0$) and at $x = 1 \pm \sqrt{2}$ (where $f(1 \pm \sqrt{2}) = 1$).
- **Dessin (b4)**: Belyi function $f(x) = \frac{(x-1)^4}{16x^2}$.
- It is intriguing to see that all preimages in $\mathbb{P}_1$ live in the extension field $\mathbb{Q}(\sqrt{2}) \in \bar{\mathbb{Q}}$ of the rational field $\mathbb{Q}$.

Recovering an octahedron: index 6 in G

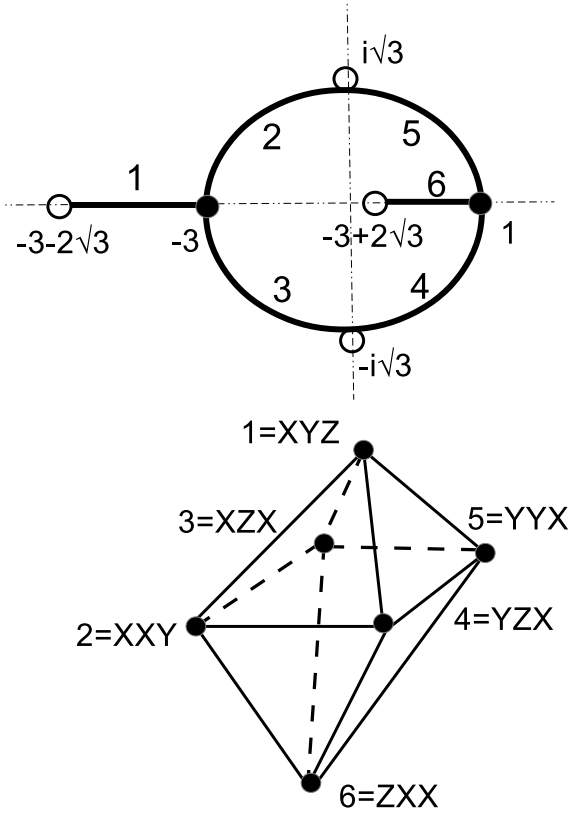

- A *dessin* (b) for the octahedron shown in (a).
  $P = \langle g_0, g_1 \rangle = \langle (1,2,3)(4,5,6), (2,4)(3,5) \rangle \cong A_4$; $s = (2,4,2,0)$;
  cycles:$=[3^2, 2^2 1^2, 3^2]$. Belyi function $f(x) = -\frac{1}{64x^3}(x-1)^3(x+3)^3$.

Identifying commutation for cosets and for observables: contextuality

- The key point is that, not only there should exist a **bijection** between a **point-line geometry** G_m stabilized by a dessin $\mathcal{D}$ and the **point-line geometry** occuring in a set of quantum observables (quantum observables as cosets), but the commutation structure in both cases should also correspond (mutually commuting operators on a line as commuting cosets).
- While the commutator for observables A and B is that for a ring: $[A, B] = AB - BA$, the commutator for the representative of two cosets a and b is the group theoretical one: $(a, b) = a^{-1}b^{-1}ab$. We identify a contextual geometry as one where at least one line of l points/cosets of the geometry fails to satisfy $(a_1, a_1, \ldots, a_l) = e$.

  The smallest index contextual geometry is recognized to be a 3×3-grid.

Recovering an octahedron

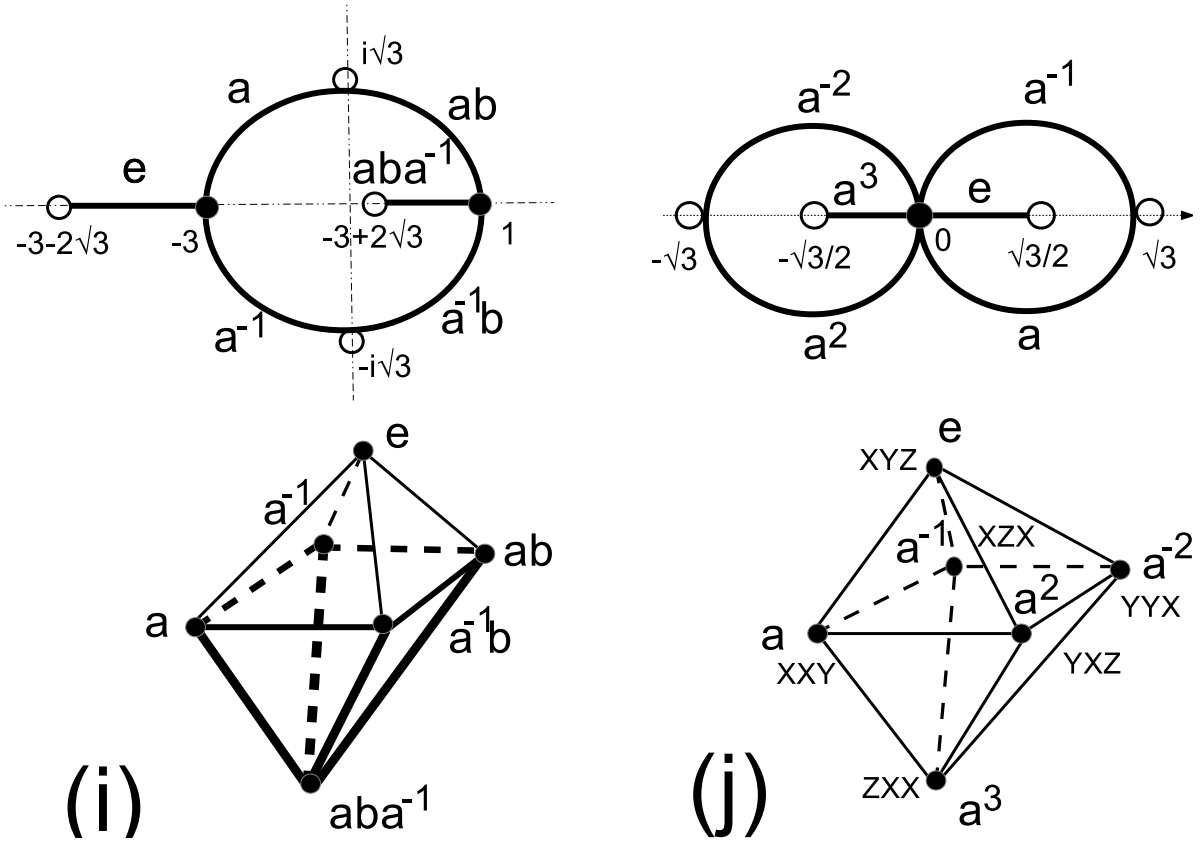

- (i) A contextual hypermap stabilizing the octahedron with the corresponding coset labelling.

  (j) A non-contextual map stabilizing the octahedron.

Two Belyi functions for the octahedron

- The **Belyi curve** for P_1 in (i) is

$$f_1(x) = -\frac{1}{64x^3}(x-1)^3(x+3)^2.$$

Take the derivative $f_1'(x) = 3(x-1)^2(x+3)^2(x^2+3)/(64x^3)$. The **critical points are black points** at $x = 1$ and $x = -3$ (where the valency is 3) and **white points** at $x = \pm i\sqrt{3}$ (where the valency is 2). Then, solving $f_1(x) = 0$, one gets $x = 1$ and -3 (black points) while solving for $f_1(x) = 1$ one gets the critical (white) points at $x = \pm i\sqrt{3}$ and the real (white) points at $x = -3 \pm 2\sqrt{3}$. The solutions of the equation $f_1(x) = \infty$ are $x = 0$ and $x = \infty$, they correspond to the center of the faces.

- The **Belyi curve** for P_2 in (j)

$$f_2(x) = \frac{4}{27}\frac{x^6}{(x^2-1)^2}.$$

index	name	vertices	edges	triangles	squares
3	2-simplex (triangle)	3	3	1	0
4	3-simplex (tethahedron)	4	6	4	0
	square/quadrangle	4	4	0	1
5	4-simplex (5-cell)	5	10	10	0
6	5-simplex	6	15	20	0
	3-**orthoplex (octahedron)**	6	12	8	3
	bipartite graph $K(3,3)$	6	9	0	9
7	6-simplex	7	21	35	0
	Fano plane (7_3)	7	21	7	0
8	7-simplex	8	28	56	0
	4-**orthoplex** (16-**cell**)	8	24	32	6
	completed cube $K(4,4)$	8	16	0	36
	stellated octahedron	8	12	8	0
9	8-simplex	9	36	84	0
	Hesse $(9_4 12_3)$	9	36	12	0
	tripartite graph $K(3,3,3)$	9	27	27	27
	Pappus (9_3)	9	27	9	27
	(3×3)-grid	9	18	6	9
10	9-simplex	10	45	120	0
	5-**orthoplex**	10	40	80	10
	bipartite graph $K(5,5)$	10	25	0	100
	Mermin's pentagram	10	30	30	15
	Petersen graph	10	15	0	0
	Desargues (10_3)	10	30	10	15
11	10-simplex	11	55	165	0
12	11-simplex	12	66	220	0
	6-**orthoplex**	12	60	160	15
	bipartite graph $K(6,6)$	12	36	0	255
	threepartite graph $K(4,4,4)$	12	48	64	108
	fourpartite graph $K(3,3,3,3)$	12	54	0	54

Small connected point-line incidence geometries induced by *dessins d'enfants*.

Small non-contextual geometries

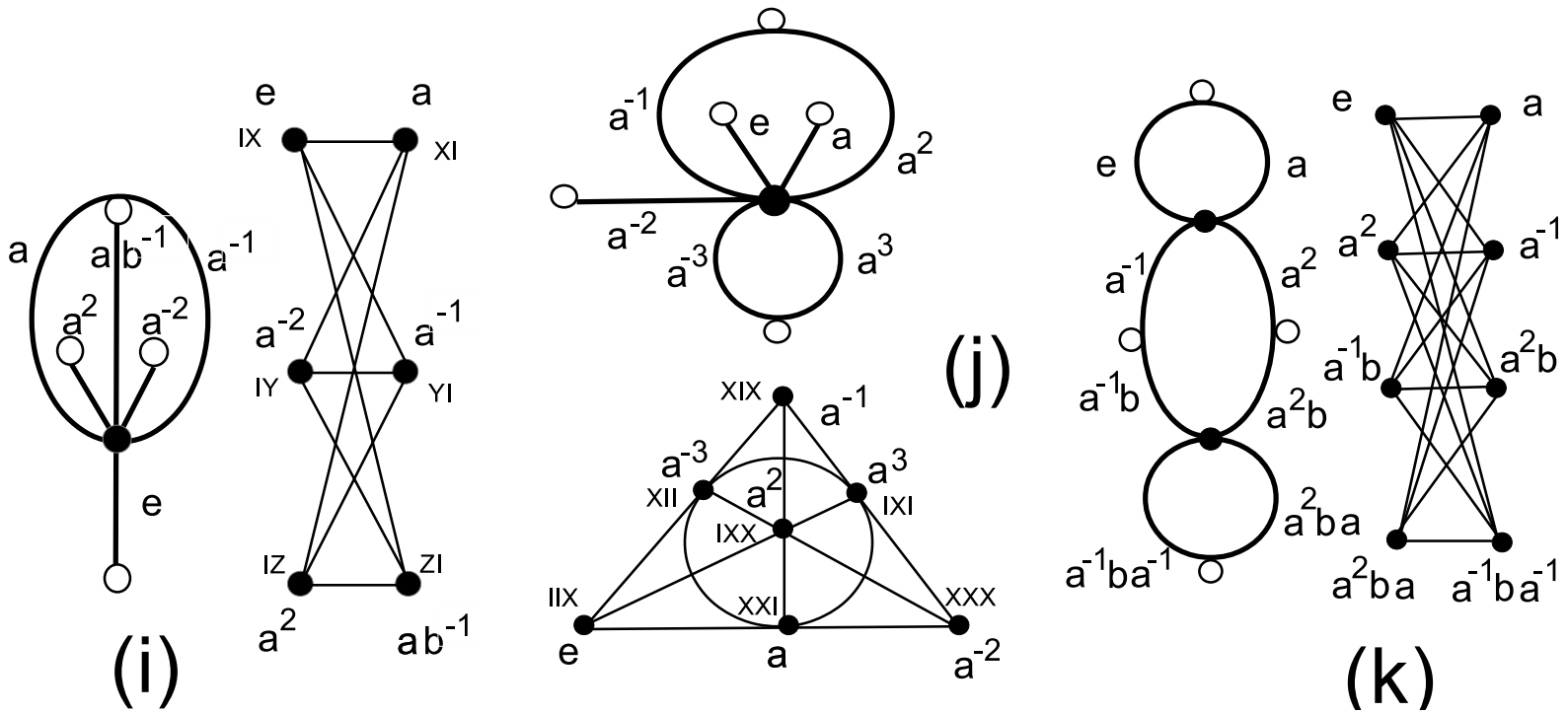

- (i) A non-contextual hypermap stabilizing the bipartite graph $K(3,3)$,
  (j) A non-contextual map/dessin stabilizing the Fano plane,
  (k) A non-contextual map/dessin stabilizing the bipartite graph $K(4,4)$.

Small contextual geometries: Mermin's square and pentagram

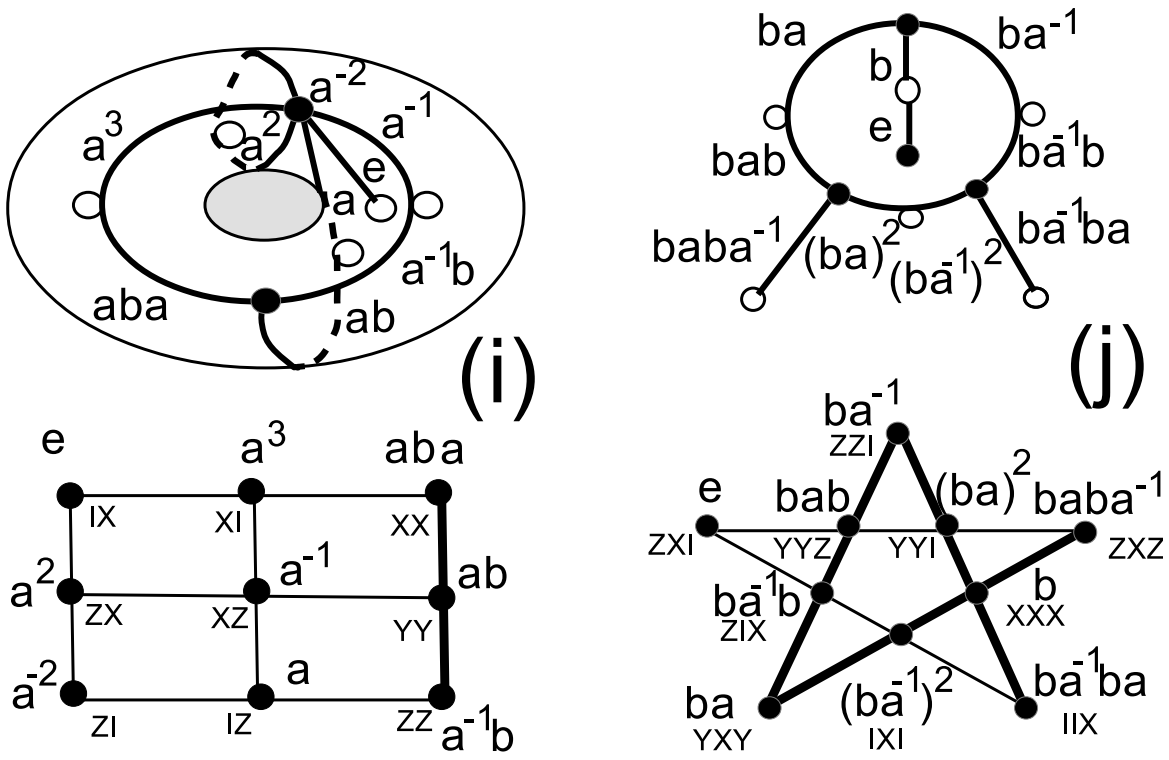

- (i) A contextual dessin stabilizing the Mermin square. The right hand side column is defective as in the original proof of Kochen-Specker theorem. (j) A contextual dessin stabilizing Mermin pentagram. The thick lines are defective.

Contextuality in maximum sets of commuting observables

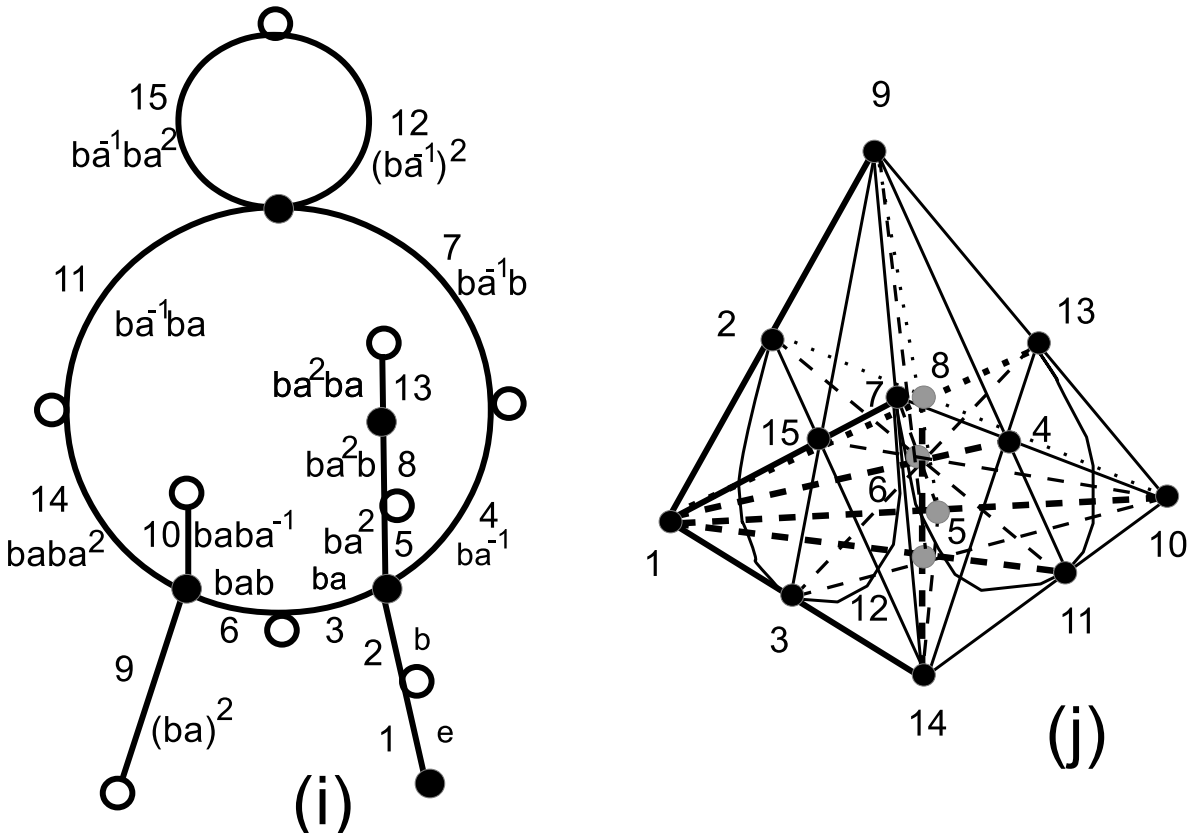

- (i) A contextual dessin stabilizing the projective space $PG(3,2)$. (ii) The projective space $PG(3,2)$ as a model of a 4-qubit maximal commuting set. A few triads inside are not drawn. Thick lines are commuting.
- And similarly $PG(2^n-1)$, $n>3$, for maximal sets of $(n+1)$-qubits.

Geometry [13]	l	u	l/u	$\log_2(h)$	Remark
$GQ(2,1)$	6	5	1.2	4	Mermin square
$GQ(2,2)$	15	3	5	5	two-qubit commutation
$GQ(2,4)$	45	5	9	6	black-hole/qubit analogy
$GH(2,1)$	14	2	7	8	in the dual of $GH(2,2)$ [14]
$GO(2,1)$	30	2	15	16	in $GO(2,4)$ [15]
$GH(2,2)$	63	3	**21**	14	3-qubit contextuality
dual of $GH(2,2)$	63	4	**15.75**	14	id

Geometric contextuality measure l/u (l the number of lines and u the number of them with mutually commuting cosets) for a few generalized polygons compared $\log_2(h)$ with h the number of geometric hyperplanes within the selected geometry.

[13] A Tits generalized polygon (or generalized n-gon) is a point-line incidence structure whose incidence graph has diameter n and girth $2n$

[14] D. Frohard and, P. Johnson, Geometric hyperplanes in generalized hexagons of order $(2,2)$, *Comm. Alg.* **22** 773 (1994).

[15] B. De Bruyn, The uniqueness of a certain generalized octagon of order $(2,4)$, Preprint 2011.

Recovering the generalized hexagon $GH(2,2)$ and its dual

We look at the **conjugacy classes of index** 63 of the group

$$\Gamma = \left\langle \rho_0, \rho_1, \rho_2 | \rho_2^2 = \rho_1^4 = (\rho_1\rho_2)^7 = (\rho_1, \rho_2)^6 = \rho_0\rho_1\rho_2 = 1 \right\rangle$$

and select the two corresponding to a dessin of permutation group P isomorphic to $S_3 \wr S_3$. There are just **two dessins** satisfying this requirement. The **first dessin** is of genus 0, signature $(21, 35, 9, 0)$. One finds three non isomorphic subgroups stabilizing a pair of elements of P, there are isomorphic to $\mathbb{Z}_6$ or D_4, or $\mathbb{Z}_2^3 \rtimes \mathbb{Z}_2^2$. The last one stabilizes the geometry of **the split Cayley hexagon** $GH(2,2)$.
The second dessin is of genus 1, signature $(18, 36, 9, 1)$. Again one finds three non isomorphic subgroups stabilizing a pair of elements of P, there are isomorphic to $\mathbb{Z}_6$ or D_4, or is the extraspecial group E_{32}^+. The latter group stabilizes **the dual of** $GH(2,2)$.

Recovering the generalized hexagon $GH(2,2)$: index 63 in C_2^+

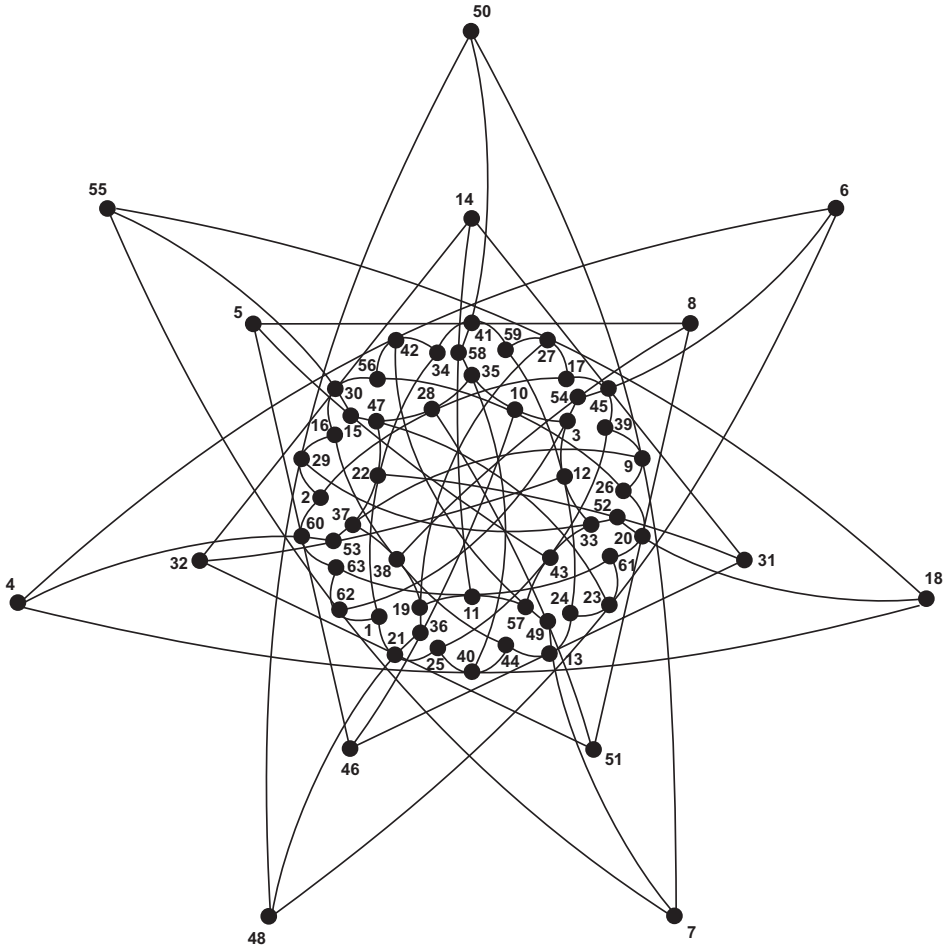

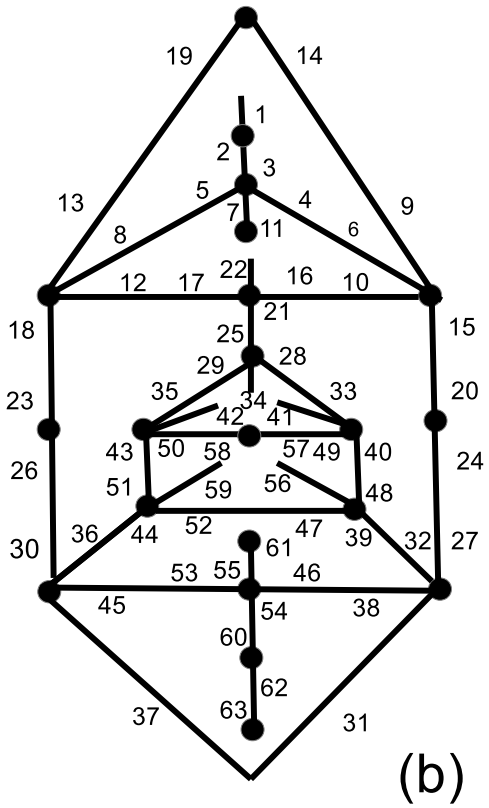

- A *dessin* for the generalized hexagon $GH(2,2)$.

Recovering a generalized hexagon: index 63 in C_2^+

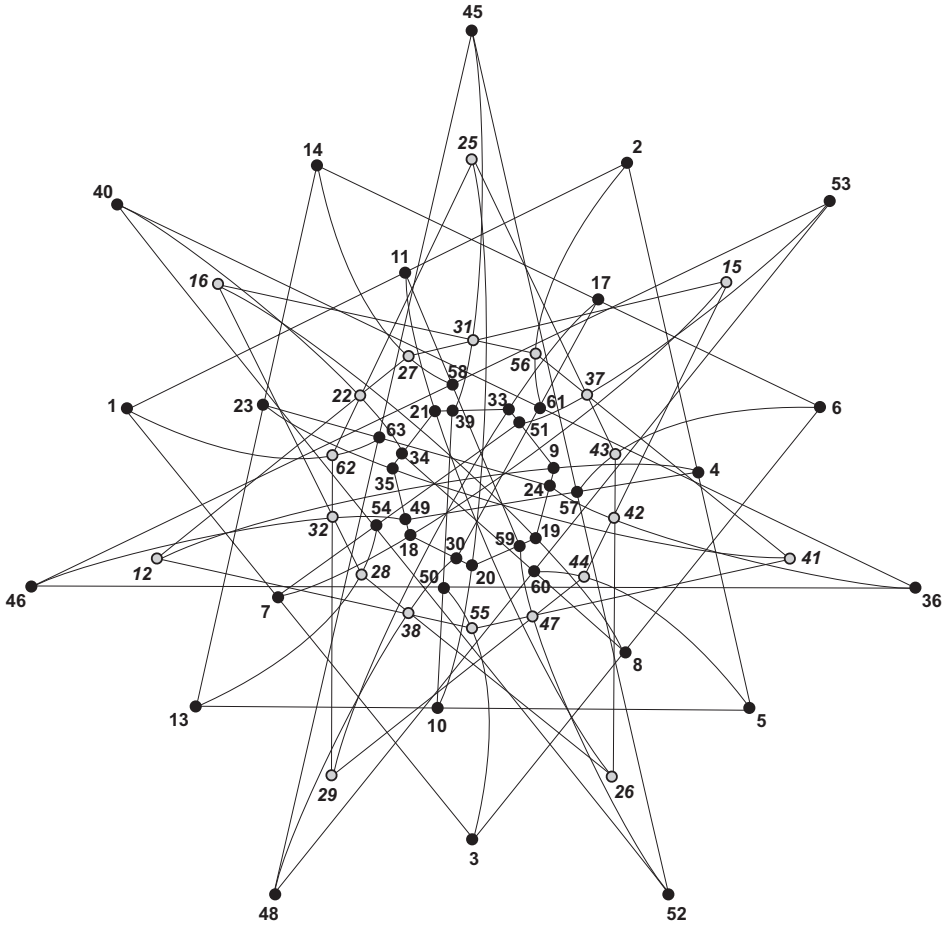

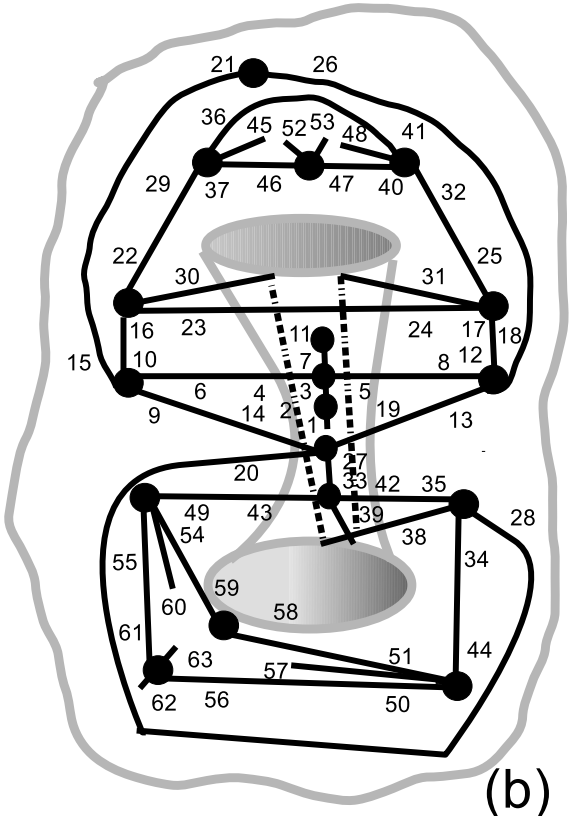

- A *dessin* for the dual of the generalized hexagon $GH(2,2)$.

Conclusion

- A striking comparison between the commutativity of quantum observables and that of cosets of subgroups of the two-generator free group. This parallel allowed us to propose **a new definition of contextuality** based on the coset structure of Grothendieck's **dessins d'enfants**, in good correspondance with the standard quantum one.
- In particular, geometric contextuality in small generalized polygons starting with the (3×3)-grid was investigated. Further work may focus on identifying and quantifying contextuality in **higher size** geometries.
- Since a complex algebraic curve defined over the field $\bar{\mathbb{Q}}$ of algebraic numbers [that is a Belyi function $f(x)$] is attached to any dessin d'enfant $\mathcal{D}$, it is expected that **the contextuality criterion features specific curves** through the action of the group of automorphisms $\mathrm{Gal}(\bar{\mathbb{Q}}/\mathbb{Q})$ of the field $\bar{\mathbb{Q}}$ (the absolute Galois group) on dessins that would be helpful to recognize.